International Journal of Research
Available at https://edupediapublications.org/journals
e-ISSN: 2348-6848
p-ISSN: 2348-795X
Volume 05 Issue 12
April 2018

Solar PV-Powered SRM for EV system with Fuzzy Logic Controller

Bhasuru. Santhoshi & M. Sai Ganesh
M.Tech Student Scholar Department of Electrical & Electronics Engineering Baba Institute of Technology & Sciences
P.M.Palem, Visakhapatnam (Dt), A.P, India.
E-Mail: santoshi.b92@gmail.com
HOD, Assistant Professor Department of Electrical & Electronics Engineering Baba Institute of Technology & Sciences
P.M.Palem, Visakhapatnam (Dt), A.P, India.
E-Mail: saiganesh229@gmail.com

Abstract:
This paper presents the use of fuzzy logic control (FLC) for switched reluctance motor (SRM) speed. Switched Reluctance Motors (SRM) has a wide range of industrial applications because of their advantages over conventional AC/DC Drives. This is due to simple construction, ruggedness and inexpensive manufacturing potential. Various methods have used and applied to control SRM speed generally, the PV-fed EV has a similar structure to the hybrid electrical vehicle, whose internal combustion engine (ICE) is replaced by the PV panel. The PV has different characteristics to ICEs, the maximum power point tracking (MPPT) and solar energy utilization are the unique factors for the PV-fed EVs. In order to achieve low cost and flexible energy flow modes, a low cost tri-port converter is proposed in this paper to coordinate the PV panel, SRM and battery. The FLC performs a PI-like control strategy, giving the current reference variation based on speed error and its change. The performance of the drive system was evaluated through MATLAB/SIMULINK software.

Key Words: Electric vehicles, photovoltaic's (PV), power flow control, switched reluctance motors (SRMs), tri-port converter, Fuzzy Logic Controller.

I. INTRODUCTION

Photovoltaic Generators (PV) provide a clean and unlimited source of energy. As part of an ongoing project on low-cost PV powered Electrical Vehicles, a control system is evaluated here for a specific configuration, based on PV panels that power a Switched Reluctance Motor, using independent controllers for maximizing the power supply and optimizing the operation of the motor [1-3]. In this paper the simulink model for the speed control of switched reluctance motor is carried out by using different speed controllers [4]. The simulink models is designed for P, PI & Fuzzy logic controller separately and their performance result is been compared [5]. The Switched Reluctance Motor is an electric motor which runs by a reluctance torque. For industrial application very high speed of 50,000 rpm motor is used [6]. The speed controllers applied here are based on conventional P& PI Controller and the other one is AI based Fuzzy Logic Controller [7].

The PI Controller proportional integral controller) is a most special case of the PID controller in which the derivative of the error is not being used [8]. Fuzzy logic controller is a most intelligent controller which uses a fuzzy logic to process the input [9]. Fuzzy logic is a many valued logic which is much like a human reasoning [10]. In the industrial control FLC has various applications, particularly where this conventional control design techniques are very difficult to apply [11]. A comprehensive reviews has done for SRM machine modelling, design and simulation and analysis and control.

To provide the maximum possible power in varying conditions, the control system aims to regulate the PV generators so that they are always at the Maximum PowerPoint (MPP) (which changes with the values of solar radiation and panel temperature and with the characteristics of the load connected to the PV) [12]. Therefore, a Maximum Power Point Tracking (MPPT) strategy is used in order to obtain the maximum available power from the panel [13]. Many methods have been developed to determine Maximum Power Point Tracking (MPPT): This paper considers the problem of coupling these energy sources to power an electrical motor in an off-grid application [14]. When a SRM load is supplied from the PV generator via a SEPIC converter then the duty cycle is controlled using a specific MPPT controller [15]. In this study, the converter duty cycle is calculated and adjusted in order to maximize power operation of the whole installation.

Generally, the PV-fed EV has a similar structure to the hybrid electrical vehicle, whose internal combustion engine (ICE) is replaced by the PV panel. The PV-fed EV system is illustrated in Fig.1. Its key components include an off-board charging station, a PV, batteries and power converters. In order to decrease the energy conversion processes, one approach is to redesign the motor to include some on-board charging functions. For instance, paper designs a 20-kW split-phase PM motor for EV charging, but it suffers from high harmonic contents in the back electromotive force (EMF). Another

International Journal of Research
Available at https://edupediapublications.org/journals
e-ISSN: 2348-6848
p-ISSN: 2348-795X
Volume 05 Issue 12
April 2018

solution is based on a traditional SRM. Paper achieves on-board charging and power factor correction in a 2.3-kW SRM by employing machine windings as the input filter inductor. The concept of modular structure of driving topology is proposed in paper. Based on intelligent power modules (IPM), a four-phase half bridge converter is employed to achieve driving and grid-charging. Although modularization supports mass production, the use of half/full bridge topology reduces the system reliability (e.g. shoot-through issues). Paper develops a simple topology for plug-in hybrid electrical vehicle (HEV) that supports flexible energy flow. But for grid charging, the grid should be connected to the generator rectifier that increases the energy conversion process and decreases the charging efficiency. Nonetheless, an effective topology and control strategy for PV-fed EVs is not yet developed. Because the PV has different characteristics to ICEs, the maximum power point tracking (MPPT) and solar energy utilization are the unique factors for the PV-fed EVs.

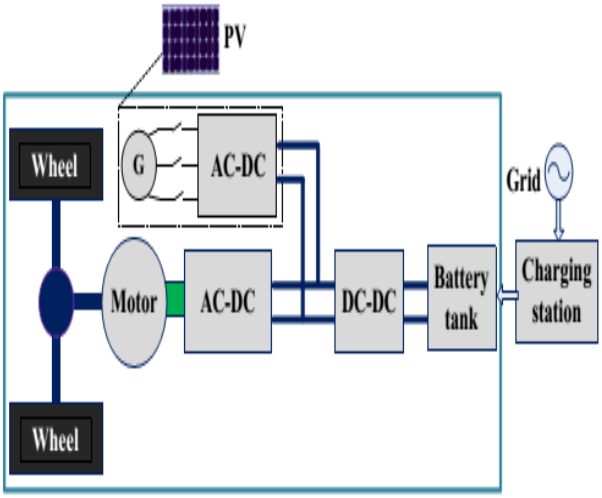

Fig.1 PV-fed hybrid electrical vehicle

II. TOPOLOGY AND OPERATIONAL MODES

A. Proposed topology and working modes

The proposed Tri-port topology has three energy terminals, PV, battery and SRM. They are linked by a power converter which consists of four switching devices (S0~S3), four diodes (D0~D3) and two relays, as shown in Fig.2 [26]. By controlling relays J1 and J2, the six operation modes are supported, as shown in Fig. 3; the corresponding relay actions are illustrated in Table I. In mode 1, PV is the energy source to drive the SRM and to charge the battery. In mode 2, the PV and battery are both the energy sources to drive the SRM. In mode 3, the PV is the source and the battery is idle. In mode 4, the battery is the driving source and the PV is idle. In mode 5, the battery is charged by a single-phase grid while both the PV and SRM are idle. In mode 6, the battery is charged by the PV and the SRM is idle.

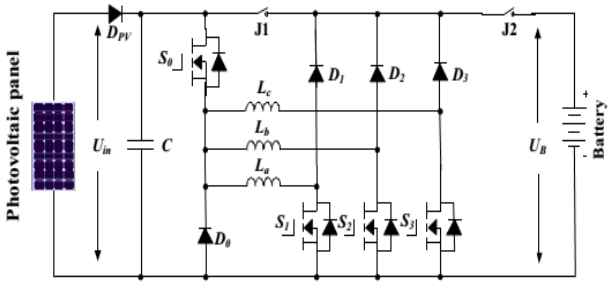

Fig.2. The proposed Tri-port topology for PV-powered SRM drive

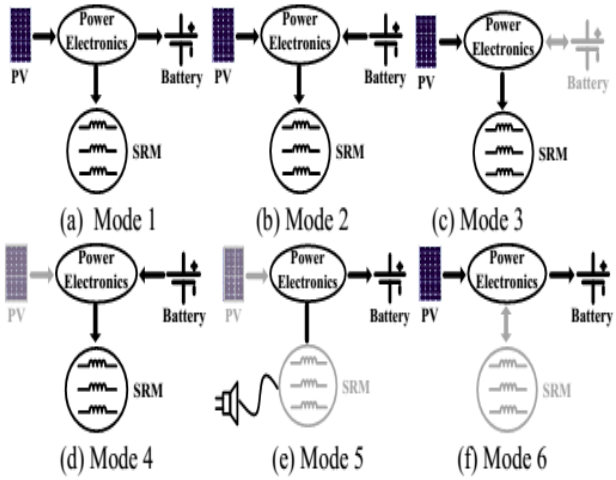

Fig.3. Six operation modes of the proposed Tri-port topology

TABLE 1 J1 and J2 Actions under Different Modes

Mode	J1 and J2
1	J1 turn-off; J2 turn-on
2	J1 and J2 turn-on
3	J1 turn-on; J2 turn-off
4	J1 and J2 turn-on
5	J1 and J2 turn-on
6	J1 turn-off; J2 turn-on

B. Driving modes

Operating modes 1~4 are the driving modes to provide traction drive to the vehicle.

(1) Mode 1

International Journal of Research
Available at https://edupediapublications.org/journals
e-ISSN: 2348-6848
p-ISSN: 2348-795X
Volume 05 Issue 12
April 2018

At light loads of operation, the energy generated from the PV is more than the SRM needed; the system operates in mode 1. The corresponding operation circuit is shown in Fig.4 (a), in which relay J1 turns off and relay J2 turns on. The PV panel energy feed the energy to SRM and charge the battery; so in this mode, the battery is charged in EV operation condition.

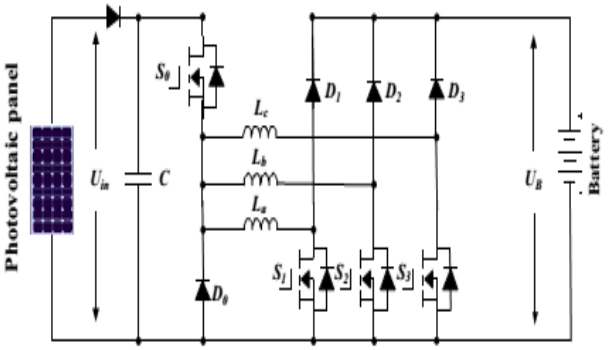

(a) Operation circuit under mode 1

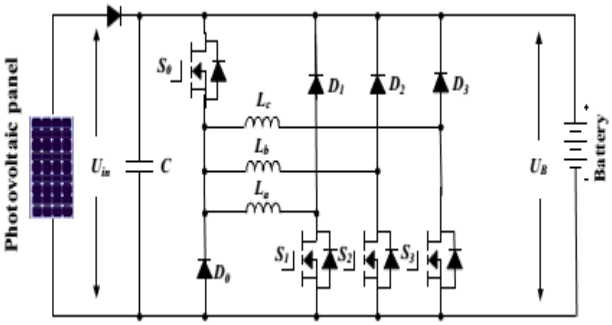

(b) Operation circuit under mode 2

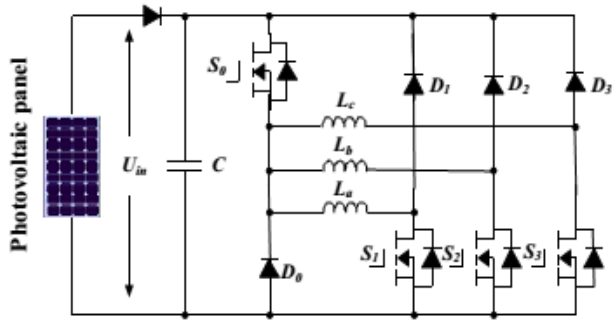

(c) Operation circuit under mode 3

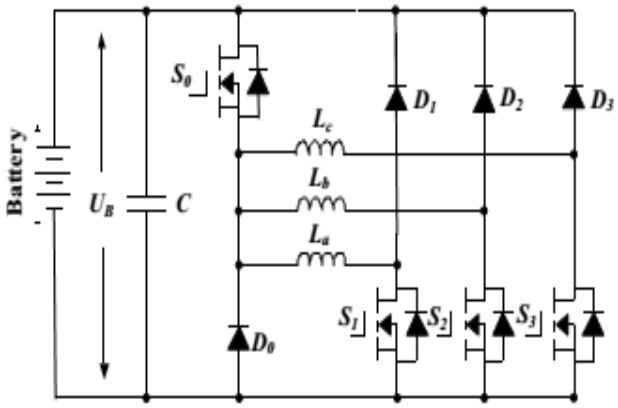

(d) Operation circuit under mode 4

Fig.4 The equivalent circuits under driving modes

(2) Mode 2

When the SRM operates in heavy load such as uphill driving or acceleration, both the PV panel and battery supply power to the SRM. The corresponding operation circuit is shown in Fig.4(b), in which relay J1 and J2 are turned on.

(3) Mode 3

When the battery is out of power, the PV panel is the only energy source to drive the vehicle. The corresponding circuit is shown in Fig.4(c). J1 turns on and J2 turns off.

(4) Mode 4

When the PV cannot generate electricity due to low solar irradiation, the battery supplies power to the SRM. The corresponding topology is illustrated in Fig.4(d). In this mode, relay J1 and J2 are both conducting.

C. Battery charging modes

Operating modes 5 and 6 are the battery charging modes.

(5) Mode 5

When PV cannot generate electricity, an external power source is needed to charge the battery, such as AC grid. The corresponding circuit is shown in Fig.5(a). J1 and J2 turns on. Point A is central tapped of phase windings that can be easily achieved without changing the motor structure. One of the three phase windings is split and its midpoint is pulled out, as shown in Fig.5(a). Phase windings La1 and La2 are employed as input filter inductors. These inductors are part of the drive circuit to form an AC-DC rectifier for grid charging.

(6) Mode 6

When the EV is parked under the sun, the PV can charge the battery. J1 turns off; J2 turns on. The corresponding charging circuit is shown in Fig.5(b).

International Journal of Research
Available at https://edupediapublications.org/journals
e-ISSN: 2348-6848
p-ISSN: 2348-795X
Volume 05 Issue 12
April 2018

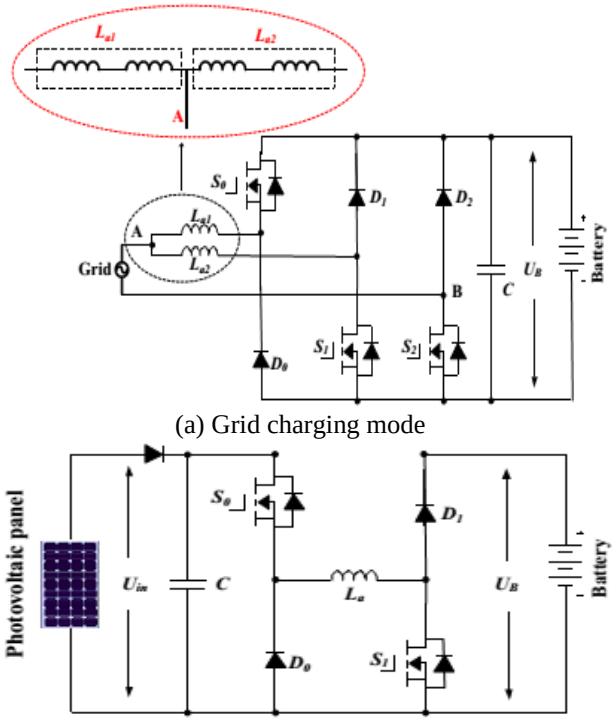

(a) Grid charging mode

(b) PV source charging mode

Fig.5 Equivalent circuits of charging condition modes

III. Control Strategy under Different Modes

In order to make the best use of solar energy for driving the EV, a control strategy under different modes is designed.

B. Single source driving mode

According to the difference in the power sources, there are PV-driving; battery-driving and PV and battery parallel fed source. In a heavy load condition, the PV power cannot support the EV, mode 2 can be adopted to support enough energy and make full use of solar energy. Fig.6(a) shows the equivalent power source; the corresponding PV panel working points is illustrated in Fig.6(b). Because the PV is paralleled with the battery, the PV panel voltage is clamped to the battery voltage UB. In mode 2, there are three working states: winding excitation, energy recycling and freewheeling states, as shown in Fig.7. Modes 3 and 4 have similar working states to mode 2. The difference is that the PV is the only source in mode 3 while the battery is the only source in mode 4.

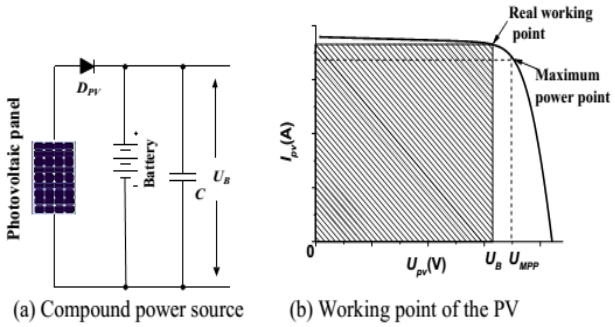

(a) Compound power source (b) Working point of the PV

Fig.6 Power supply at mode 2

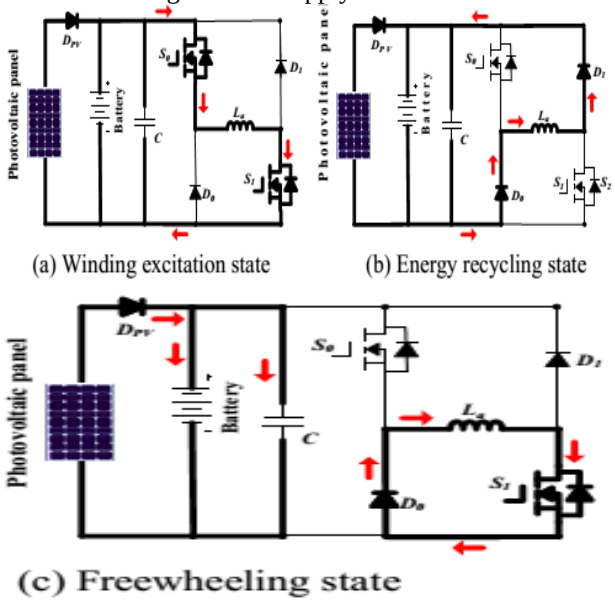

(a) Winding excitation state (b) Energy recycling state

Fig.7 Working states at mode 2

Neglecting the voltage drop across the power switches and diodes, the phase voltage is given by

$$U_{\text{in}} = R_k i_k + \frac{d\psi(i_k,\theta_r)}{dt}$$

$$= R_k i_k + L_k \frac{di_k}{dt} + i_k \omega_r \frac{dL_k}{d\theta_r}, \quad k = a,b,c \qquad (1)$$

where U_{in} is the DC-link voltage, k is phase a, b, or c, R_k is the phase resistance, i_k is the phase current, L_k is the phase inductance, θr is the rotor position, $\psi(i_k, \theta_r)$ is the phase flux linkage depending on the phase current and rotor position, and ωr is the angular speed. The third term in Eq.1 is the back electromotive force (EMF) voltage given by

$$e_k = i_k \omega_r \frac{dL_k}{d\theta_r} \qquad (2)$$

Hence, the phase voltage is found by

International Journal of Research
Available at https://edupediapublications.org/journals
e-ISSN: 2348-6848
p-ISSN: 2348-795X
Volume 05 Issue 12
April 2018

$$U_k = R_k i_k + L_k \frac{di_k}{dt} + e_k \quad (3)$$

In the excitation region, turning on S0 and S1 will induce a current in phase a winding, as show in Fig.7(a). Phase a winding is subjected to the positive DC bus voltage.

$$+U_{in} = R_k i_k + L_k \frac{di_k}{dt} + e_k \quad (4)$$

When S0 is off and S1 is on, the phase current is in a freewheeling state in a zero voltage loop, as shown in Fig.3.7(c), the phase voltage is zero.

$$0 = R_k i_k + L_k \frac{di_k}{dt} + e_k \quad (5)$$

In the demagnetization region, S0 and S1 are both turned off, and the phase current will flow back to the power supply, as show in Fig.7(b). In this state, the phase winding is subjected to the negative DC bus voltage, and the phase voltage is

$$-U_{in} = R_k i_k + L_k \frac{di_k}{dt} + e_k \quad (6)$$

In single source driving mode, the voltage-PWM control is employed as the basic scheme, as illustrated in Fig.8. According to the given speed ω*, the voltage-PWM control is activated at speed control.

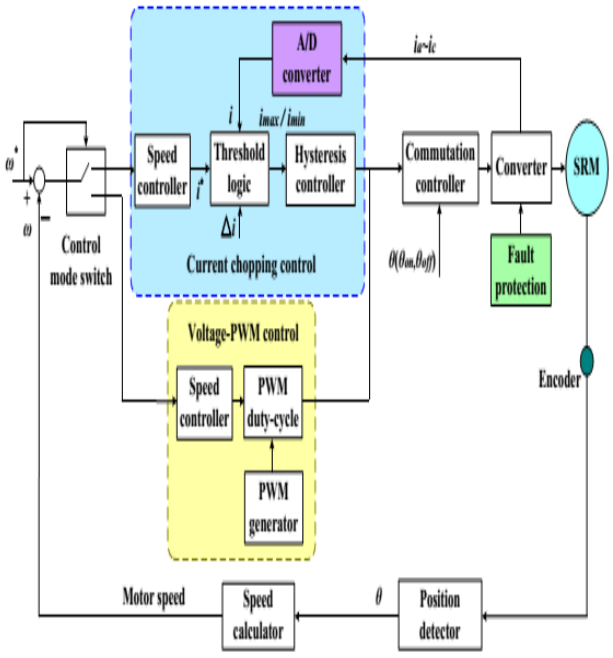

Fig.8 SRM control strategy under single source driving mode

B. Driving-charging hybrid control strategy

In the driving-charging hybrid control, the PV is the driving source and the battery is charged by the freewheeling current, as illustrated in drive mode 1. There are two control objectives: maximum power point tracking (MPPT) of the PV panel and speed control of the SRM.

The dual-source condition is switched from a PV-driving mode. Firstly, the motor speed is controlled at a given speed in mode 3. Then, J2 is tuned on and J1 is off to switch to mode 1. By controlling the turn-off angle, the maximum power of PV panel can be tracked.

There are three steady working states for the dual-source mode (mode 1), as shown in Fig.9. In Fig.9(a), S0 and S1 conduct, the PV panel charges the SRM winding to drive the motor; In Fig.9(b), S0 and S1 turn off; and the battery is charged with freewheeling current of the phase winding. Fig.9(c) shows a freewheeling state.

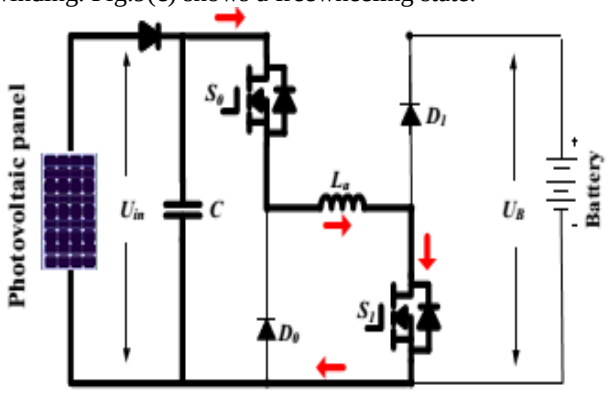

(a) Winding exciting state

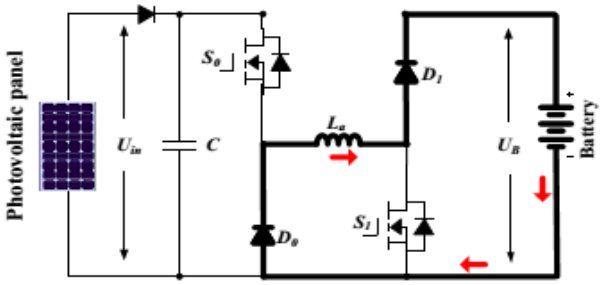

(b) Battery charging state

International Journal of Research
Available at https://edupediapublications.org/journals
e-ISSN: 2348-6848
p-ISSN: 2348-795X
Volume 05 Issue 12
April 2018

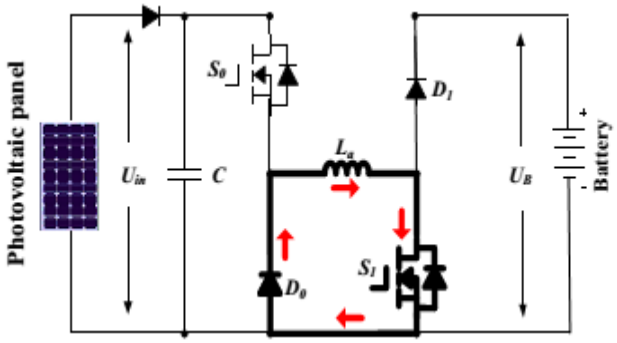

(c) Freewheeling state

Fig.9 Mode 1 working states

Fig.10 is the control strategy under driving-charging mode. In Fig.10, θon is the turn on angle of SRM; θoff is the turn-off angle of SRM. By adjusting turn-on angle, the speed of SRM can be controlled; the maximum power point tracking of PV panel can be achieved by adjusting turn-off angle, which can control the charging current to the battery.

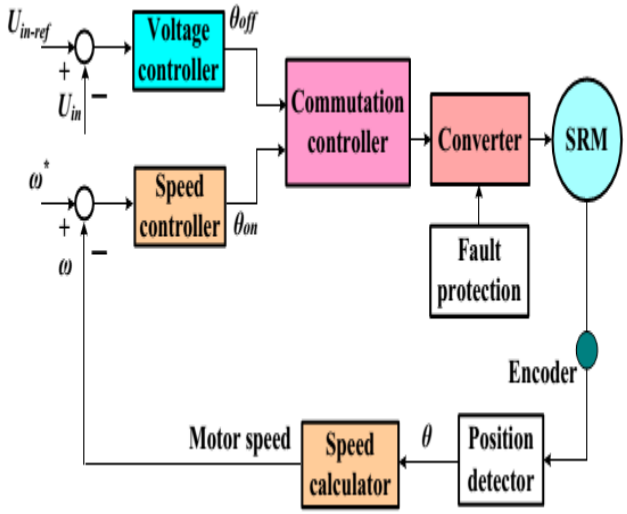

Fig.10. Control strategy under driving-charging mode (mode 1)

C. Grid-charging control strategy

The proposed topology also supports the single-phase grid charging. There are four basic charging states and S0 is always turned off. When the grid instantaneous voltage is over zero, the two working states are presented in Fig.11(a) and (b). In Fig.11(a), S1 and S2 conduct, the grid voltage charges the phase winding La2, the corresponding equation can be expressed as Eq.7; In Fig.11(b), S1 turns off and S2 conducts, the grid is connected in series with phase winding to charges the battery, the corresponding equation can be expressed as Eq.8.

$$U_{grid} = L_{a2} \cdot \frac{di_{grid}}{dt} \quad (7)$$

$$U_B - U_{grid} = L_{a2} \cdot \frac{di_{grid}}{dt} \quad (8)$$

When the grid instantaneous voltage is below zero, the two working states are presented in Fig.11 (c) and (d). In Fig.11(c), S1 and S2 conduct, the grid voltage charges the phase winding La1 and La2, the corresponding equation can be expressed as Eq. (9); In Fig.11(d), S1 keeps conducing and S2 turns off, the grid is connected in series with phase winding La1 and La2 to charges the battery, the corresponding equation can be expressed as Eq.10.

$$U_{grid} = \frac{L_{a1} + L_{a2}}{L_{a1} \cdot L_{a2}} \cdot \frac{di_{grid}}{dt} \quad (9)$$

$$-U_B - U_{grid} = \frac{L_{a1} + L_{a2}}{L_{a1} \cdot L_{a2}} \cdot \frac{di_{grid}}{dt} \quad (10)$$

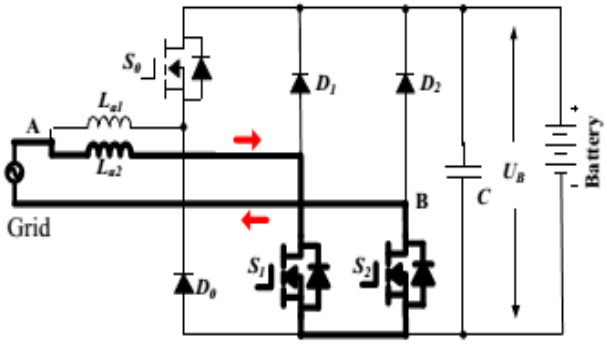

(a) Grid charging state 1 (Ugrid>0)

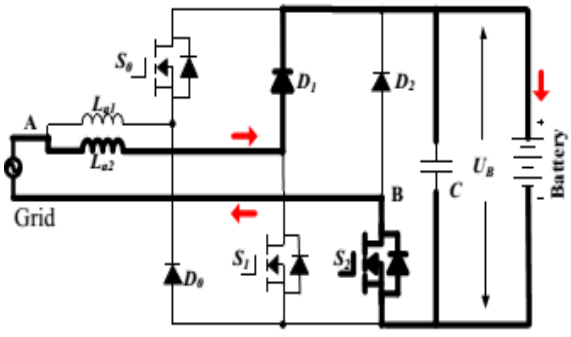

(b) Grid charging state 2 (Ugrid>0)

International Journal of Research
Available at https://edupediapublications.org/journals
e-ISSN: 2348-6848
p-ISSN: 2348-795X
Volume 05 Issue 12
April 2018

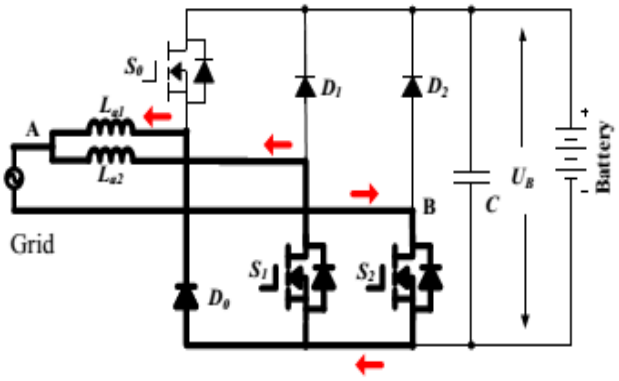

(c) Grid charging state 3 (Ugrid<0)

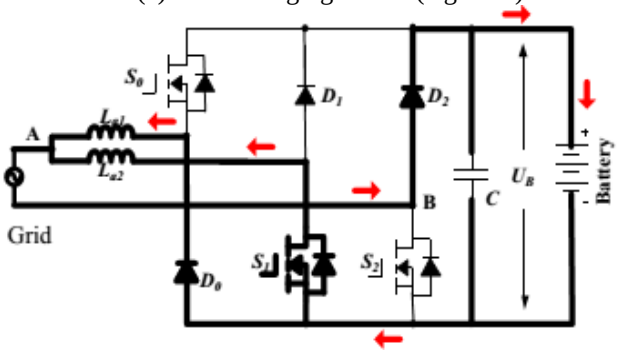

(d) Grid charging state 4 (Ugrid<0)

Fig.3.11 Mode 5 charging states

In Fig.12, Ugrid is the grid voltage; by the phase lock loop (PLL), the phase information can be got; Iref_grid is the given amplitude of the grid current. Combining sinθ and Iref_grid, the instantaneous grid current reference iref_grid can be calculated. In this mode, when Ugrid> 0, the inductance is La2; when Ugrid< 0, the inductance is paralleled La1 and La2; in order to adopt the change in the inductance, hysteresis control is employed to realize grid current regulation. Furthermore, hysteresis control has excellent loop performance, global stability and small phase lag that makes grid connected control stable.

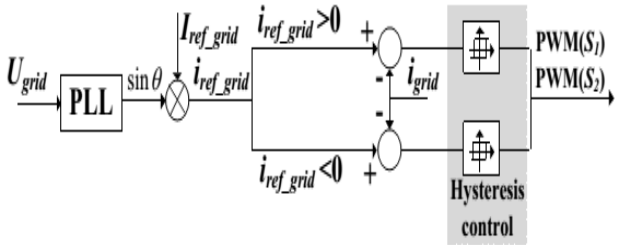

Fig.12 Grid-connected charging control (Mode 5)

D. PV-fed charging control strategy

In this mode, the PV panel charges the battery directly by the driving topology. The phase windings are employed as inductor; and the driving topology can be functioned as interleaved Buck boost charging topology. For one phase, there are two states, as shown in Fig.13(a) and (b). When S0 and S1 turn on, the PV panel charges phase inductance; when S0 and S1 turns off, the phase inductance discharges energy to battery. According to the state-of-charging (SoC), there are three stages to make full use of solar energy and maintain battery healthy condition, as illustrated in Fig.13 (c). During stage 1, the corresponding battery SoC is in 0~SoC1, the battery is in extremely lack energy condition, the MPPT control strategy is employed to make full use of solar energy. During stage 2, the corresponding battery SoC is in SoC1~ SoC2, the constant voltage control is adapted to charging the battery. During stage 3, the corresponding battery SoC is in SoC2~1, the micro current charging is adapted. In order to simplify the control strategy, constant voltage is employed in PV panel MPPT control.

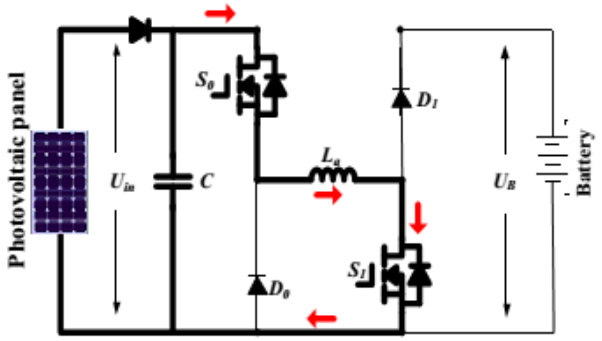

(a) Phase inductance charging

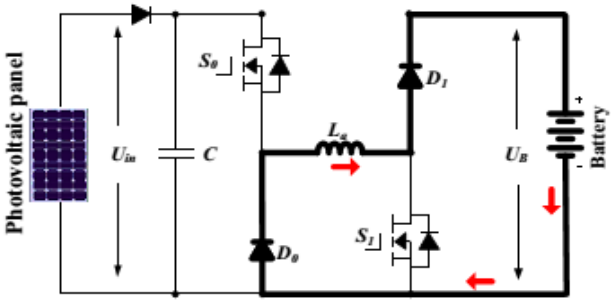

(b) Battery charging

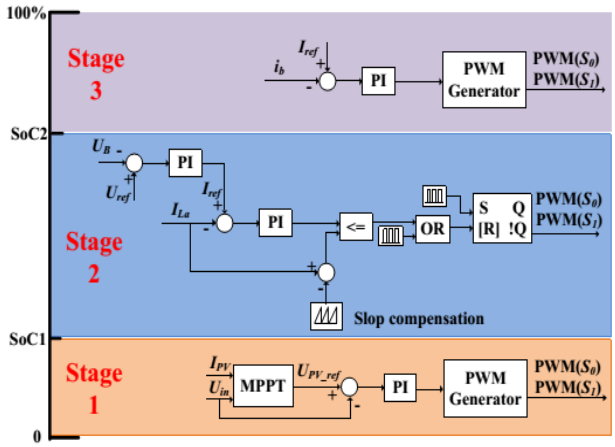

(c) Charging control strategy.

Fig.13 Mode 6 charging states and control strategy.

IV. DESIGN OF A FUZZY CONTROLLER

The difficulty regarding the PI controller gain is the fine tuning of the controller so as to achieve the optimal operation of the task. The major drawback of the PI controller is faced when the process is nonlinear and also when the system is having oscillations. Considering all these facts, a fuzzy logic controller was implemented. A fuzzy controller can work in linear as well as in nonlinear design parameters. FL requires some numerical parameters in order to operate such as what is considered significant error and significant rate-of-change-of error, but exact values of these numbers are usually not critical unless very responsive performance is required in which case empirical tuning would determine them.

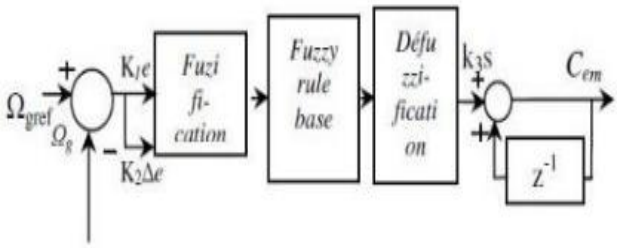

Fig.14 Fuzzy Logic Controller

FL requires some numerical parameters in order to operate such as what is considered significant error and significant rate-of-change-of-error, but exact values of these numbers are usually not critical unless very responsive performance is required in which case empirical tuning would determine them. For example, a simple temperature control system could use a single temperature feedback sensor whose data is subtracted from the command signal to compute "error" and then time-differentiated to yield the error slope or rate-of change-of-error, hereafter called "error-dot".

V. MATLAB/SIMULATION RESULTS

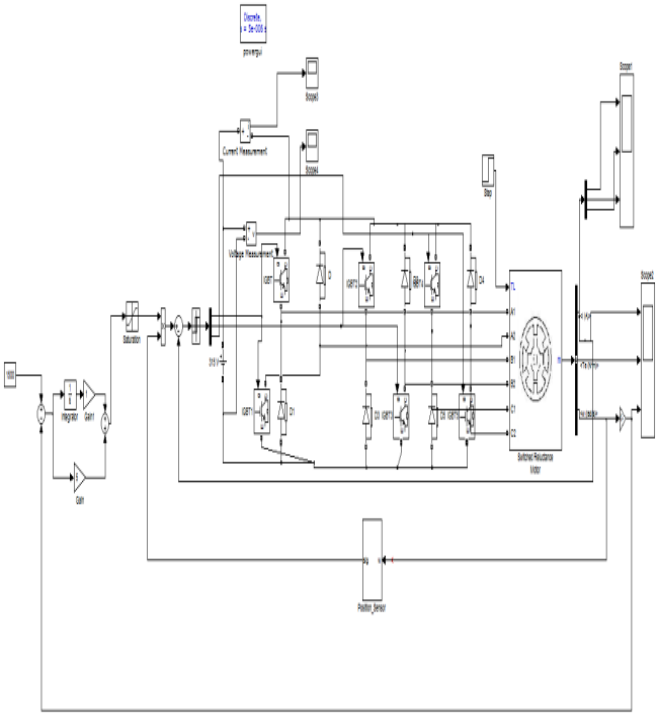

Fig.15 SRM drive model diagram

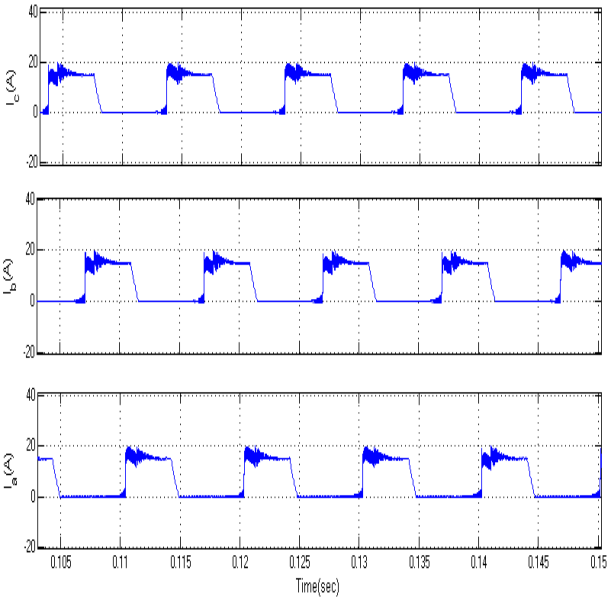

International Journal of Research
Available at https://edupediapublications.org/journals
e-ISSN: 2348-6848
p-ISSN: 2348-795X
Volume 05 Issue 12
April 2018

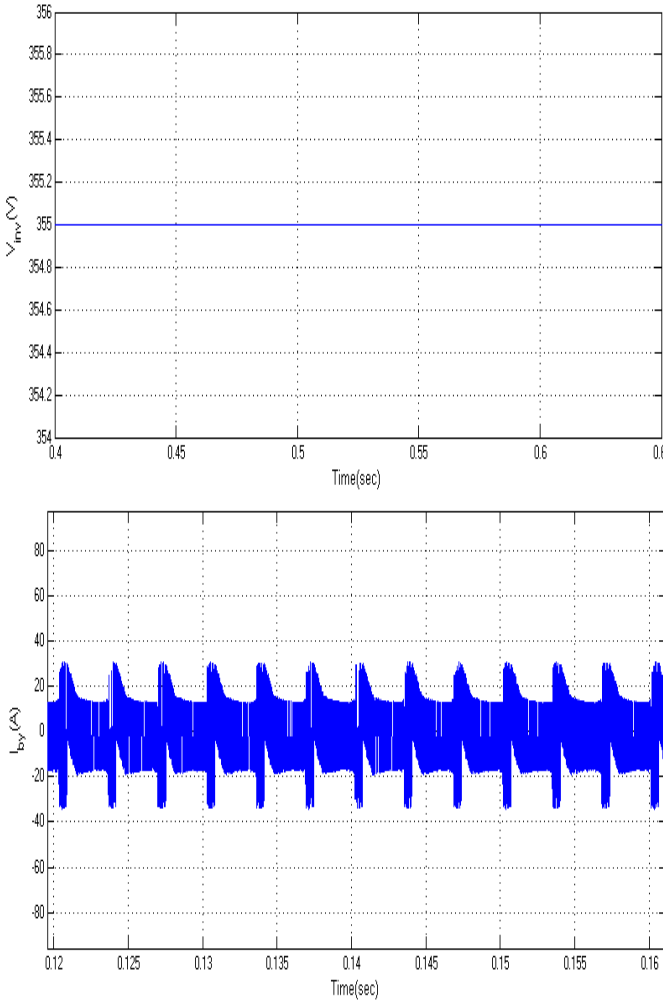

(a) Simulation results of driving-charging mode (mode 1)

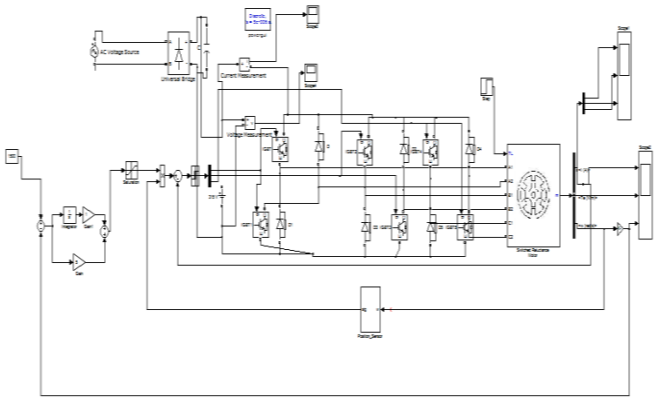

Fig.16 SRM drive model diagram

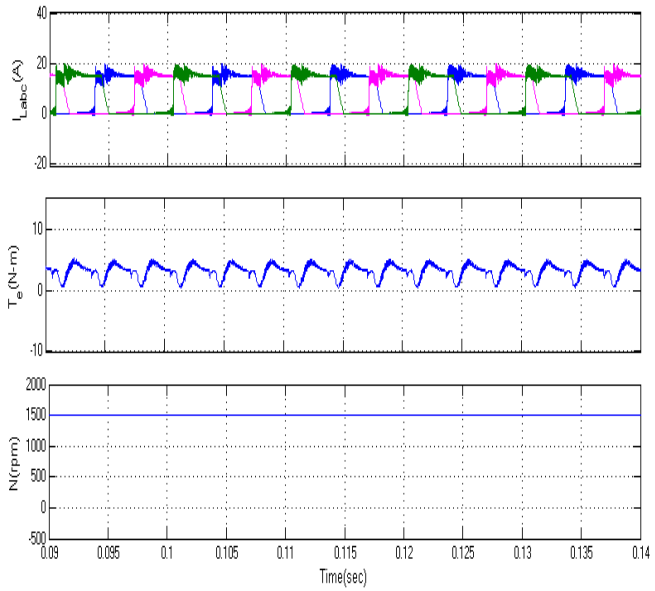

(b) Simulation results of single source driving mode (modes 3 and 4)

Fig.17 Simulation results for driving conditions at modes 1, 3 and 4.

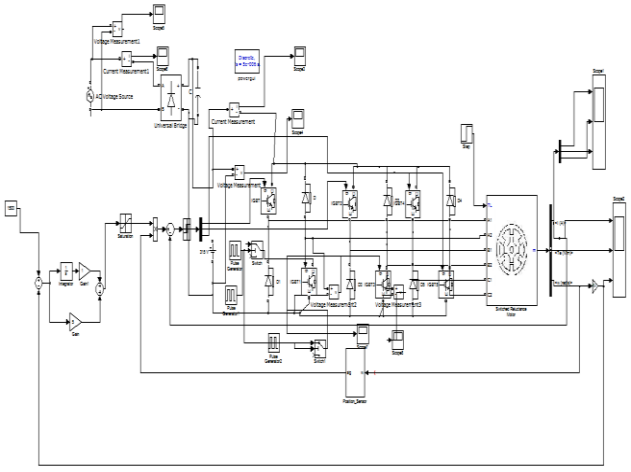

Fig.18 SRM drive model diagram

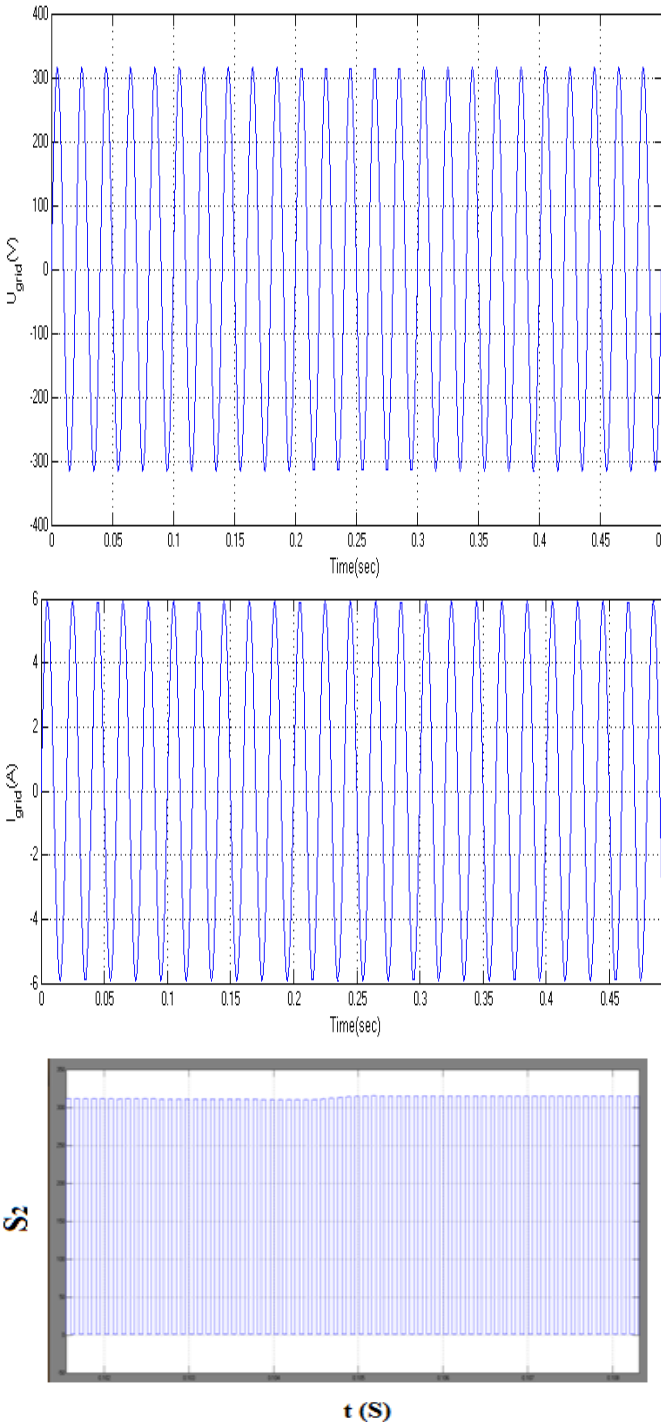

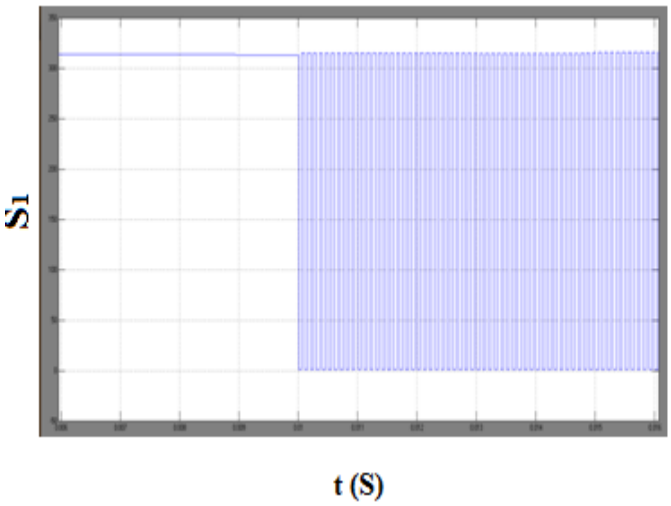

(a) Grid charging (mode 5)

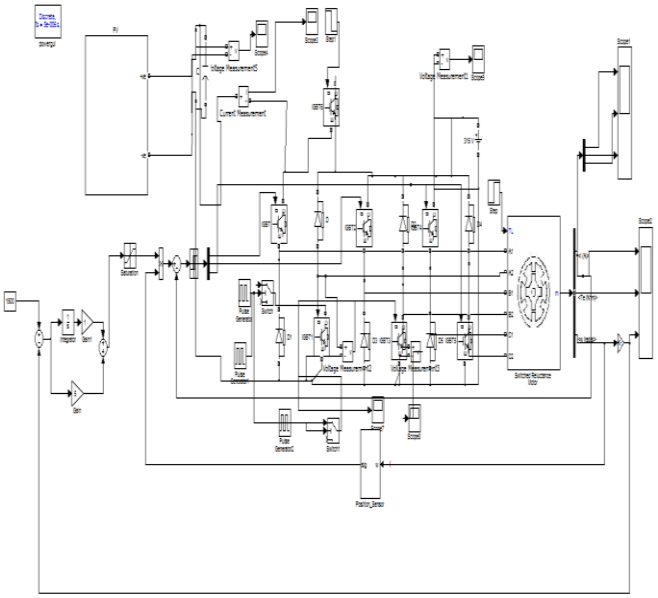

Fig.19 PV-powered SRM drive model diagram

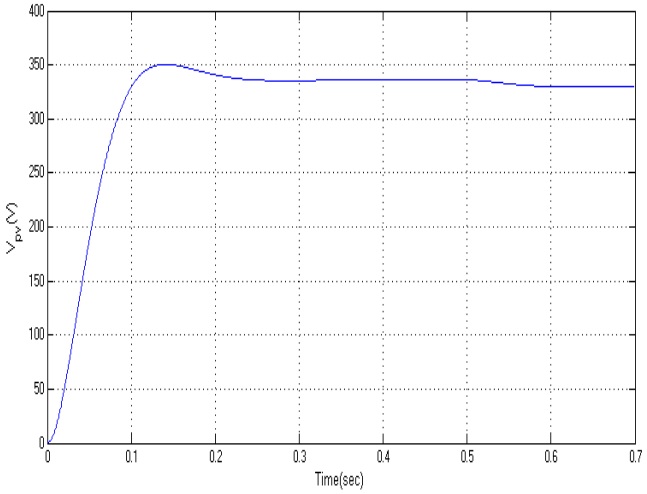

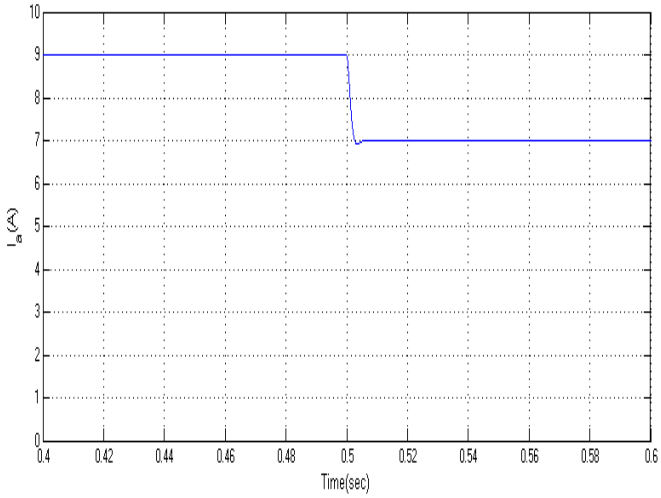

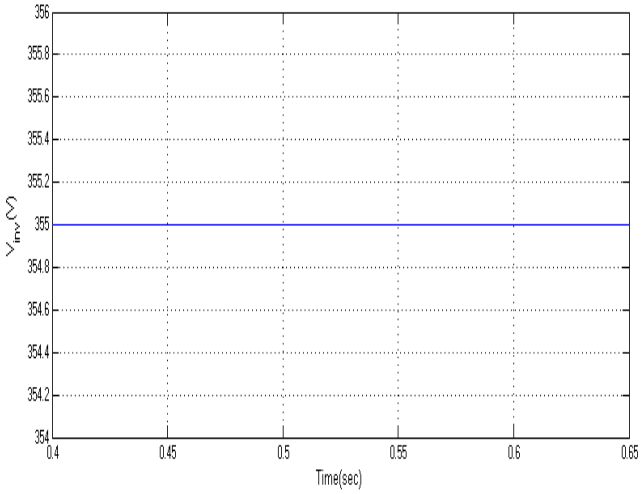

(b) PV charging mode 6 (stage 1 to stage 2)

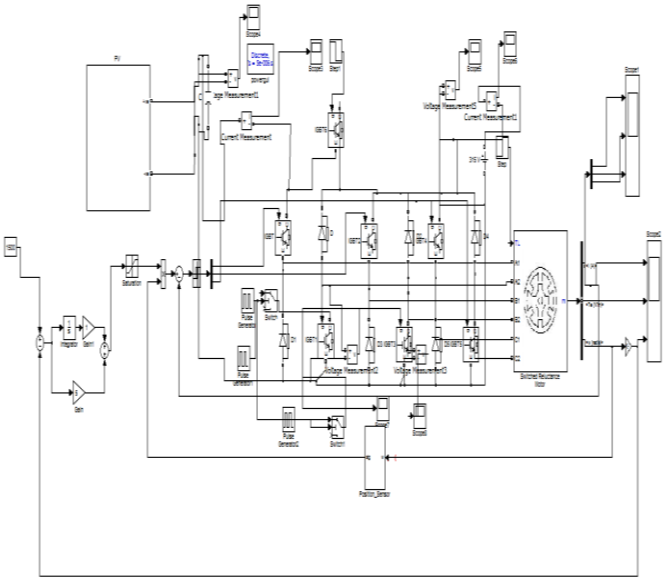

Fig.20 PV-powered SRM drive model diagram

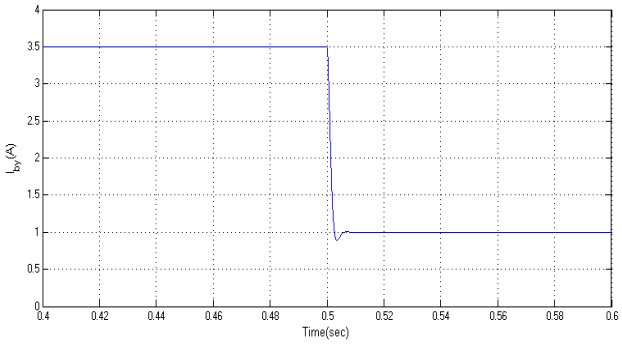

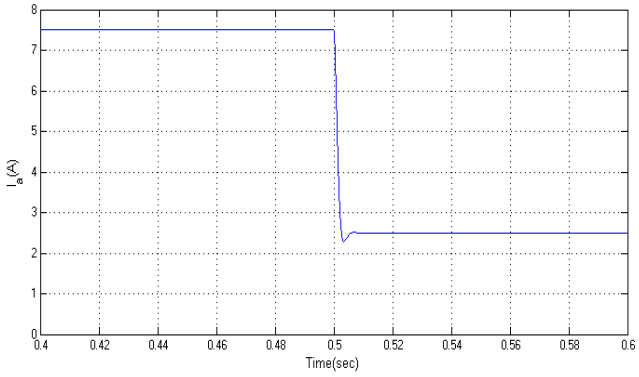

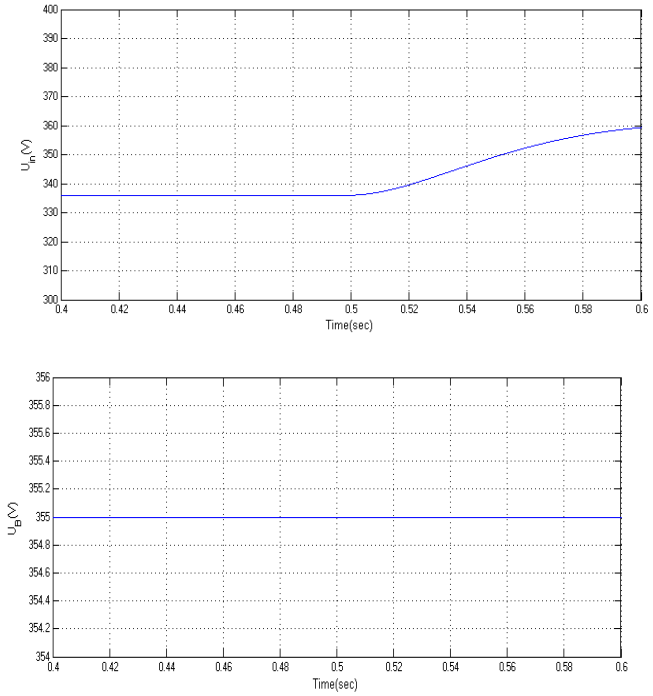

(c) PV charging mode 6 (stage 2 to stage 3)

Fig.21 simulation results for charging modes.

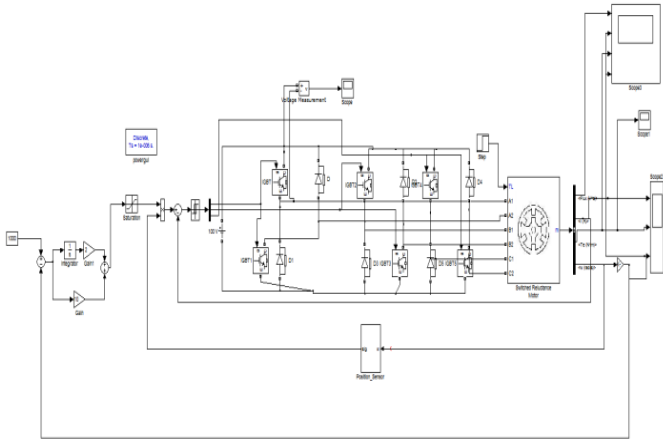

Fig.22 SRM drive model diagram With PI controller

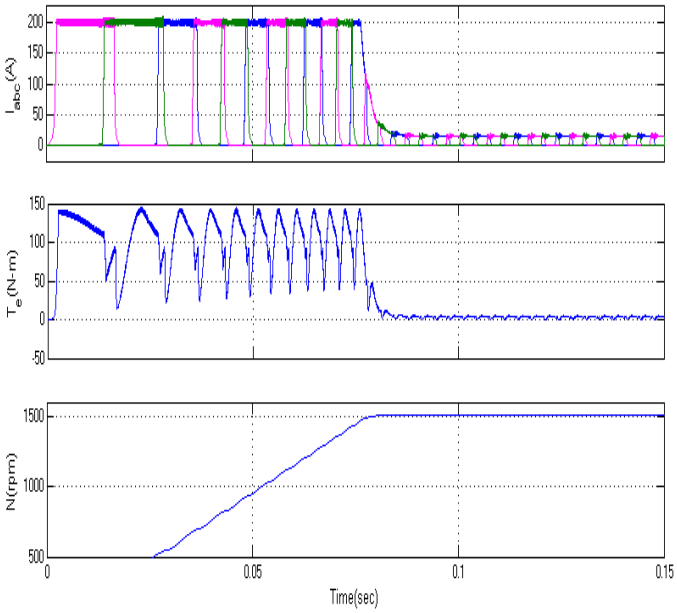

Fig.23 Flux, Current, Speed and Torque

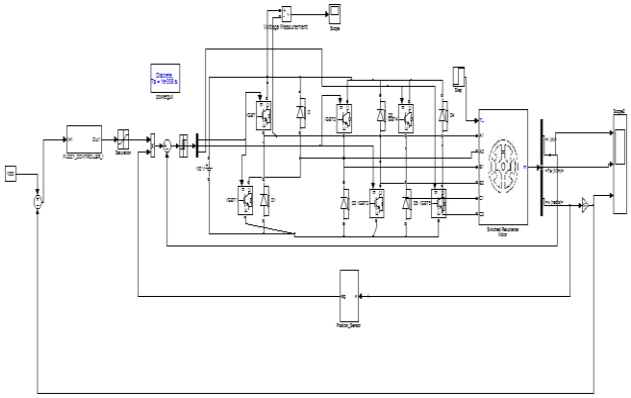

Fig.24 SRM drive model diagram With Fuzzy controller

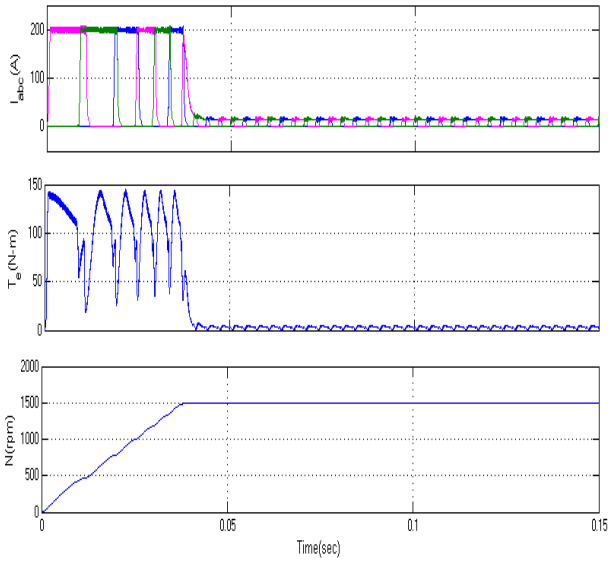

Fig.25 Current, Speed and Torque

VI. CONCLUSION

In this work the SRM dynamic performance is implemented by using MATLAB/simulink. In conventional methods the speed control of SRM motor is concluded by PI. Here it is executed with Fuzzy Logic Controller. Fuzzy Logic Controller gives the required output than the other controllers. In this proposed method the fuzzy logic controller ensure excellent reference tracking of switched reluctance motor drives. This fuzzy logic controller gives the best speed tracking without overshoot and enchances the speed regulation.

REFERENCES

[1] A. Emadi, L. Young-Joo, K. Rajashekara, "Power electronics and motordrives in electric, hybrid electric, and plug-in hybrid electric vehicles,"IEEE Trans. Ind. Electron., vol. 55, no. 6, pp. 2237-2245, Jun. 2008.

[2] B. l. K. Bose, "Global energy scenario and impact of power electronics in21st century," IEEE Trans. Ind. Electron., vol. 60, no. 7, pp. 2638-2651,Jul. 2013.

[3] J. de Santiago, H. Bernhoff, B. Ekergård, S. Eriksson, S. Ferhatovic, R.Waters, and M. Leijon,"Electrical motor drivelines in commercial allelectric vehicles: a review," IEEE Trans. Veh. Technol., vol. 61, no. 2, pp.475-484, Feb. 2012.

Ind. Electron., vol. 60, no. 9, pp. 5696- 5710, Oct. 2014.

[4] Z. Amjadi, S. S. Williamson, "Power-electronics-based solutions for plugin hybrid electric vehicle energy storage and management systems," IEEETrans. Ind. Electron., vol. 57, no. 2, pp. 608-616, Feb. 2010.

[5] A. Kuperman, U. Levy, J. Goren, A. Zafransky, and A. Savernin, "Batterycharger for electric vehicle traction battery switch station," IEEE Trans.Ind. Electron., vol. 60, no. 12, pp. 5391-5399, Dec. 2013.

[6] S. G. Li, S. M. Sharkh, F. C. Walsh, and C. N. Zhang, "Energy and batterymanagement of a plug-in series hybrid electric vehicle using fuzzy logic,"IEEE Trans. Veh. Technol., vol. 60, no. 8, pp. 3571-3585, Oct. 2011.

[7] C. H. Kim, M. Y. Kim, and G. W. Moon, "A modularized chargeequalizer using a battery monitoring IC for series-connected Li-Ion batteryStrings in electric vehicles," IEEE Trans. Power Electron., vol. 28, no. 8,pp. 3779-3787, May 2013.

[8] Z. Ping, Z. Jing, L.Ranran, T. Chengde, W. Qian, "Magneticcharacteristics investigation of an axial-axial flux compound-structurePMSM used for HEVs," IEEE Trans. Magnetics, vol. 46, no. 6, pp. 2191-2194, Jun. 2010.

[9] A. Kolli, O. Béthoux, A. De Bernardinis, E. Labouré, and G. Coquery,"Space-vector PWM control synthesis for an H-bridge drive in electricvehicles," IEEE Trans. Veh. Technol., vol.62, no.6, pp. 2441-2452, Jul.2013.

[10] S. M. Yang, and J. Y. Chen, "Controlled dynamic braking for switchedreluctance motor drives with a rectifier front end," IEEE Trans. Ind.Electron., vol. 60, no. 11, pp. 4913- 4919, Nov. 2013.

[11] B. Bilgin, A. Emadi, M. Krishnamurthy, "Comprehensive evaluation ofthe dynamic performance of a 6/10 SRM for traction application inPHEVs," IEEE Trans. Ind. Electron., vol. 60, no. 7, pp. 2564-2575, July.2013.

[12] M. Takeno, A.Chiba, N. Hoshi, S. Ogasawara, M. Takemoto, M. A.Rahman, "Test results and torque improvement of the 50-kW switchedreluctance motor designed for hybrid electric vehicles," IEEE Trans. Ind.Appl., vol. 48, no. 4, pp. 1327-1334, Jul/Aug. 2012.

[13] A. Chiba, M. Takeno, N. Hoshi, M. Takemoto, S.Ogasawara, M. A.Rahman, "Consideration of number of series turns in switched-reluctancetraction motor competitive to HEV IPMSM," IEEE Trans. Ind. Appl., vol.48, no. 6, pp. 2333-2340, Nov/Dec. 2012.

[14] I. Boldea, L. N. Tutelea, L. Parsa, and D. Dorrell, "Automotive electricpropulsion systems with reduced or no permanent magnets: an overview,"IEEE Trans.